

A novel approach to brazing C/C composite to Ni-based superalloy using alumina interlayer

Yuanxun Shen, Zhenglin Li, Chuanyong Hao, Jinsong Zhang*

Institute of Metal Research, Chinese Academy of Sciences, 72 Wenhua Road, Shenyang 110016, China

Received 8 August 2011; received in revised form 28 November 2011; accepted 11 December 2011

Available online 31 January 2012

Abstract

C/C composite was brazed to a Ni-based superalloy using an active AgCu braze with an alumina ceramic interlayer and/or a zig–zag interfacial structure between the C/C and the braze. The joint with the Al_2O_3 interlayer displayed perfectly bonded interface and ductile joint microstructure because the diffusion and chemical reactions of Ni and Ti are prevented, which in turn improved the joint strength due to the reduced residual stress. Moreover, the joint was significantly strengthened and toughened by the proposed zig–zag interfacial structure. The strengthening mechanism was attributed to the enlarged joining area, reduced residual stress and strong pinning effect of the braze spikes. A quite high bending strength of 73 MPa was obtained from the C/C-superalloy joint with the zig–zag interfacial structure.

© 2012 Published by Elsevier Ltd.

Keywords: C/C composite; Brazing; Al_2O_3 interlayer; Microstructure; Mechanical properties

1. Introduction

Carbon fibre reinforced carbon matrix composite (C/C composite) is an attractive material for thermal structural applications in aerospace, brakes and nuclear reactors due to its excellent mechanical performance at elevated temperature.^{1–3} Many such applications require joining C/C to various metals. In the past decade, C/C composite was directly joined to Ti alloy,^{4,5} and Cu-clad Mo⁶ and Ni alloy^{7,8} using the so-called active brazing method. However, the joint strength was unsatisfactory. For example, the highest strength of the C/C–Ti joints was only 25 MPa. The main problem related to C/C–metal joint is the large mismatch between their coefficients of thermal expansion (CTE), which induces great residual stresses during cooling process, and consequently deteriorates the joint strength. Thus, controlling the residual stress is of vital importance to maintaining the strength of C/C–metal joint. For this purpose, a stress relief interlayer is always utilized. Furthermore, it is noted that multiple inter-layers are more effective to reduce the residual stress than a single interlayer in ceramic–metal joint^{9–11}. In addition, a ductile joint microstructure is also important in relaxing

the residual stress through plastic deformation. However, the original ductile brazes in the reported C/C–metal joints were usually seriously hardened by the brittle compounds as produced by excessive chemical reactions, which would preclude effective stress relief and lead to weakened joint. Therefore, to control the chemical reactivity, so as to maintain the ductile structure in the joint, a diffusion barrier is always used.^{12,13}

Up to now, the mechanical strength of C/C–Ni alloy joint is rarely reported. The purpose of this work is to fabricate high strength C/C–Ni-based superalloy joint with alumina ceramic as the interlayer using a AgCu brazing alloy. A novel strengthening method by construction of a zig–zag interfacial structure between the C/C and the braze is proposed. Microstructures and mechanical properties of the C/C–superalloy joint were investigated. Influence of the alumina interlayer on the microstructure and mechanical strength of joint was studied. Strengthening mechanism of the zig–zag interfacial structure was discussed in detail as well.

2. Experimental

C/C composite used in this experiment was a semi-3D C/C composite that was prepared with carbon fibre cloth and needle felt. The metal section was a nickel-based wrought superalloy with a nominal composition of

* Corresponding author. Tel.: +86 24 23971896; fax: +86 24 23971896.
E-mail address: jshzhang@imr.ac.cn (J. Zhang).

Table 1
Summary of the different joint modes in this study.

Mode no.	Joint configuration	C/C surface condition
1	CC/AgCu/Superalloy	Flat
2	CC/AgCu/Al ₂ O ₃ /AgCu/Superalloy	Flat
3	CC/AgCu/Al ₂ O ₃ /AgCu/Superalloy	Mirco-machined

Ni–20Cr–8W–7.5Mo–2Fe–0.6Al–0.5Ti (in wt.%). The dimensions of C/C composite and superalloy samples for bending test were both 6.4 mm × 6.2 mm × 25 mm and those for metallographic examination were 10 mm × 8 mm × 5 mm and 15 mm × 10 mm × 5 mm, respectively. An alumina plate (95% purity) with size of 6.6 mm × 6.4 mm × 2 mm was employed as the interlayer in the C/C-superalloy joint. In particular, the joining surfaces of the Al₂O₃ substrate were metalized via a Mo–Mn process. A commercially available Ag–28Cu eutectic alloy foil with thickness of 250 μm was used as the filler metal. The braze foil was ground with a 400# SiC paper and afterwards cut into size of 6.4 mm × 6.2 mm for brazing. Prior to joining, both the braze foils and the superalloy samples were ultrasonically cleaned in acetone for 15 min.

In this work, three kinds of joints with different joining configurations were studied, as listed in Table 1. In joint mode 1 and 2, C/C composites with flat surfaces were used as received. The difference between mode 1 and 2 was that no alumina interlayer was used in the former. In joint mode 3, the C/C surface was mirco-machined by means of laser, resulting in a multitude of conical holes with depth of 300–1000 μm into the composite. For all C/C samples, a 10 μm thick Ti film was deposited on the joining surface by a magnetron sputtering method. In particular, for the C/C samples used in joint mode 3, a certain amount of TiH₂ powder was brushed into the laser machined holes by a simple slurry technique (suspension in ethanol). In order to promote the wettability of the braze, a Ni film of 5 μm was coated on the surface of the superalloy block. After that, the assemblies of C/C–Superalloy joint according to Table 1 were placed into a custom stainless steel jig to ensure a proper axiality of the joint during brazing. The brazing was carried out at 910 °C for 10 min in a vacuum furnace. Subsequently, the joint was furnace cooled to room temperature.

Mechanical strength of the joint was evaluated by four-point bending test on the beam shaped specimens with a cross head

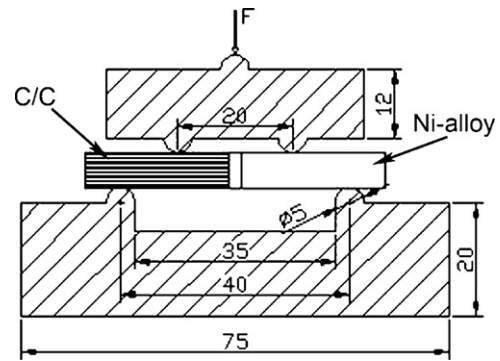


Fig. 1. Schematic of the device used for bending test.

Table 2
The EDS analysis results of the regions marked in Figs. 2–4.

Zone	Compositions (at.%)				Possible phase
	Ag	Cu	Ti	Ni	
A	–	23.2	33.7	43.1	Ti(Cu,Ni) ₂
B	50.2	3.7	46.1	–	AgTi
C	8.2	26.1	58.8	6.9	Ti ₂ Cu
D	4.7	21.7	57.8	15.8	Ti ₂ (Cu,Ni)
E	1.4	82.6	–	16	Cu[Ni, Ag]
F	93.5	6.5	–	–	Ag[Cu]
G	2.2	76.5	–	21.3	Cu[Ni, Ag]

speed of 1 mm/min. Schematic of the device used for the bending test is shown in Fig. 1. Microstructure characteristics of the joint and fracture surfaces were investigated by scanning electron microscopy (SEM) and energy dispersive X-ray spectroscopy (EDS).

3. Results and discussions

3.1. Microstructure of C/C–superalloy joint without interlayer

Typical cross-sectional SEM images of the joints in different modes are shown in Figs. 2–4. Compositions at the marked points obtained by EDS analysis are listed in Table 2. Fig. 2 shows the secondary electron (SE) image of the C/C–Superalloy joint in mode 1. The joint has a eutectic structure composed

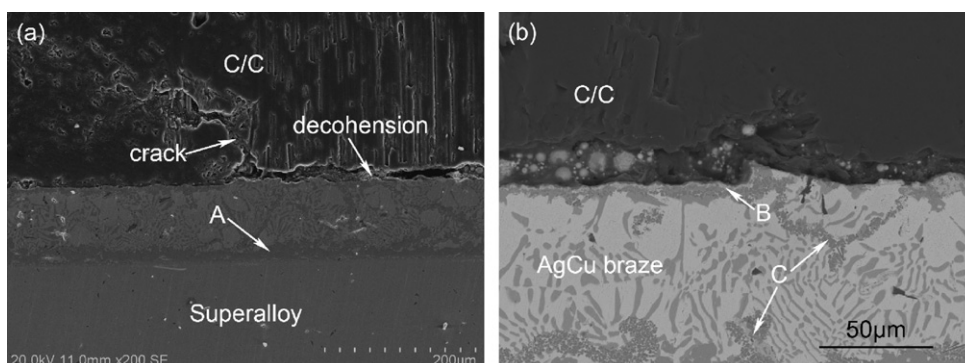


Fig. 2. Microstructure of (a) C/C–superalloy joint in mode 1 and (b) C/C–braze interface.

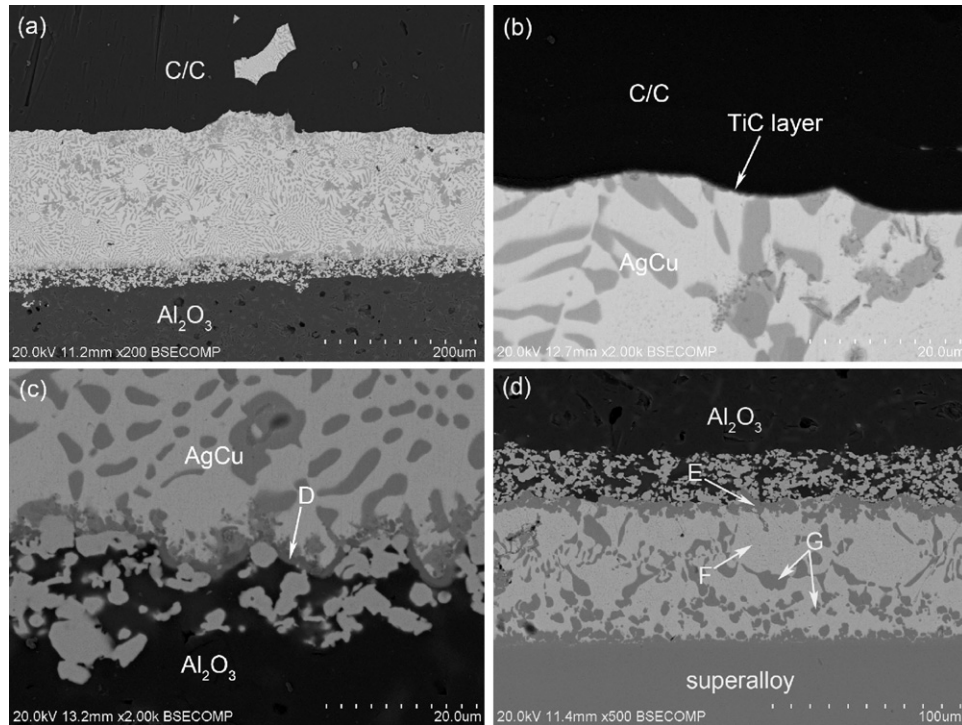


Fig. 3. SEM micrograph of (a) C/C- Al_2O_3 joint in mode 2, (b) C/C-braze interface, (c) braze/ Al_2O_3 interface, and (d) Al_2O_3 -superalloy joint.

mainly of Ag-rich and Cu-rich phases. Besides, there are quite a few intermetallic compounds, such as $\text{Ti}(\text{Cu}, \text{Ni})_2$ (point A), AgTi (point B) and Ti_2Cu (point C), in the joint zone, as noted in Fig. 2a and b, which should have resulted from the chemical reactions of Ti with Ni and Cu in the molten braze. It has been reported that the formation of brittle Ti_2Cu and $\text{Ti}(\text{Cu}, \text{Ni})_2$ phases was harmful to the joints because they may induce strong hardening effect to the braze and so forth degrade its ductility.^{14,15} As a result, cracks were prone to occur at or near the ceramic/braze interface due to the residual stress. From Fig. 2, we can clearly observe the interfacial decohesion at the CC/braze interface. Some cracks are also observed in the C/C matrix. Many studies have revealed that the difference in CTE between the ceramics and metals can cause cracks or failure due to the residual stresses.^{8,16} Our results indicate that similar problems also existed with C/C-Ni-based superalloy joint.

3.2. Microstructure of the C/C-superalloy joint with Al_2O_3 interlayer

The backscattered electron (BSE) image of the C/C- Al_2O_3 -superalloy joint in mode 2 is shown in Fig. 3. In comparison to the joint in mode 1, as shown in Fig. 3a, the C/C- Al_2O_3 joint reveals intimately contacted interface and is free of structural defects such as cracks and voids. The joint is comprised of homogeneous AgCu eutectic microstructure. A continuous reaction layer with high Ti concentration was formed at the CC/braze interface, as shown in Fig. 2b, suggesting possible formation of TiC. The Gibb's free energy change (ΔG) for TiC formation via the reaction of Ti and C at 910°C is -174 kJ/mol , which indicates that TiC formation during brazing is thermodynamically favourable. In fact, pure Ag or Cu does not wet C/C and the contact angle is very high. However, adding small amount of Ti to

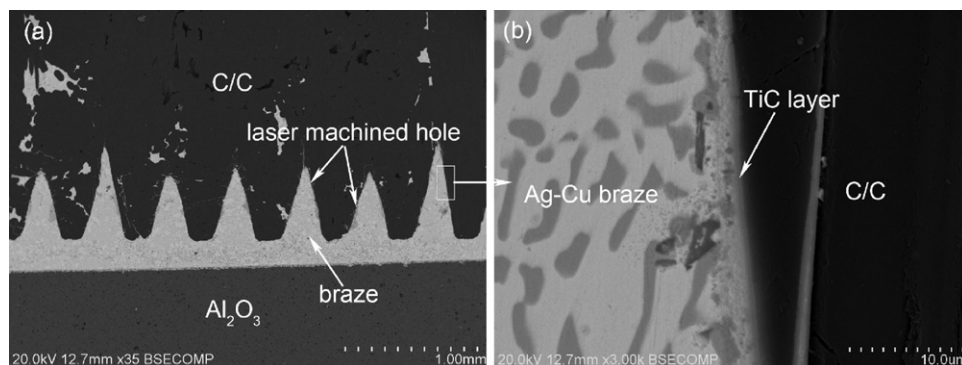


Fig. 4. SEM micrograph of (a) C/C- Al_2O_3 joint in mode 3 and (b) C/C-braze interface at location boxed in (a).

the braze has improved its wettability through the formation of carbide. The formation of TiC has been commonly observed in Ti-containing brazes/carbon systems.^{5–8} Fig. 3c shows the interface between the braze and Al₂O₃. A Ti-rich layer (marked as D) alloyed with Cu and Ni is observed, which means that sound metallurgical bonds have been obtained. The segregation of Ti to the braze/Al₂O₃ interface indicates that Ti diffused from the C/C side across the braze had reacted with Ni because of the strong chemical affinity between Ti and Ni.

Fig. 3d shows a BSE image of the Al₂O₃-superalloy joint. The wettability of the AgCu alloy on Al₂O₃ and superalloy was obviously improved in the presence of the Ni coating though without the use of active Ti. A CuNi solution layer (point E) was formed on the Al₂O₃ side. On the superalloy side, the original Ni coating disappeared due to its diffusing or dissolving into the molten braze. The joint is perfectly bonded and displays two solid solution phases, Ag[Cu] (point F) and Cu[Ni,Ag] (point E and H). The characteristics of the Al₂O₃-Hastelloy joint using a AgCuTi braze have been investigated by Asthana and co-workers¹⁷. Although their joint was defect-free, the joint microstructure was rather complex because of the extensive inter-diffusion and reactions of the active Ti with the alloying elements from metal substrate, which inevitably led to the formation of brittle compounds. Therefore, in comparison to the microstructure of Asthana's joint, our joint is more ductile due to lack of intermetallic compounds.

Fig. 4 shows typical morphology of the C/C-Al₂O₃ joint with a zig-zag interfacial structure. As seen from Fig. 4a, all the laser-machined holes have been completely filled with the braze alloy. The C/C/braze interface in the holes is well-bonded due to the formation of a TiC layer, as shown in Fig. 4b. In addition, penetration of the braze into the C/C matrix through the intrinsic open pores and cracks can be clearly observed. This infiltrated structure is beneficial since it can lead to the typical "nail effect".¹⁸ Homogeneous AgCu eutectic microstructure was obtained in this joint. We believe that this infiltrating behaviour of the braze into the laser machined holes is quite akin to the ductile phase toughening of the brittle ceramics by dispersing metal particles in them.

As seen from Figs. 2–4, the Al₂O₃ interlayer exhibits positive effect on the microstructures of the C/C-Superalloy joint. As mentioned above, the joint in mode 1 had cracks at the CC/braze interface, revealing partially bonded interface. By contrast, the joint with the Al₂O₃ interlayer was well-bonded and displayed homogeneous microstructure. No intermetallic compounds were found in the joints of C/C-Al₂O₃ and Al₂O₃-superalloy. In this study, Ti and Ni films were coated on the C/C and superalloy surfaces respectively before brazing. For the mode 1 joint, the Ni (derived from Ni coating and superalloy) dissolved extensively in melted AgCu alloy. Meanwhile, inter-diffusion and chemical reactions could take place between Ti with Ni and Cu. As a result, brittle compounds were formed during brazing. For the joint in mode 2 and 3, the consumption of Ti at the Al₂O₃ surface for bond formation and the corresponding decrease in Ti content reduced the Ti diffusion from the C/C side toward the Al₂O₃ side, which effectively prevented the formation of brittle compounds at the C/C-braze interface or in the joint zone. In addition, the

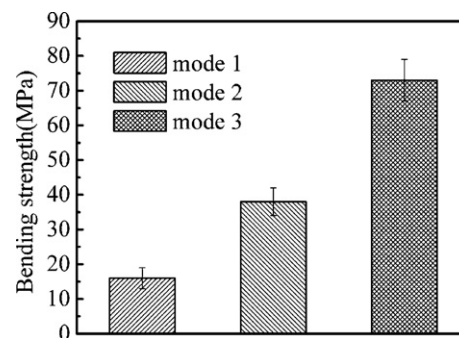


Fig. 5. Mechanical strength of the joints in different modes.

diffusion of Ni from the superalloy side to the C/C side and the migration of Ti to the superalloy side were completely prevented by the Al₂O₃ interlayer, which avoided the reactions between Ni and Ti. As a result, the interlayer leads to homogeneous and ductile microstructure in the C/C-Al₂O₃ and Al₂O₃-superalloy joints.

3.3. Mechanical strength of joints

Mechanical strengths of the joints in different modes are compared in Fig. 5. The model 1 joint only shows a bending strength of 16 MPa. This is consistent with the observed defects in this joint. However, by introducing the alumina interlayer, the mechanical strength of the C/C-Ni-based superalloy joints is obviously enhanced. The joint in mode 2 shows an average bending strength of 33 MPa. This should be due to the improved interface bonding and the elimination of brittle compounds and cracks. Moreover, the use of the zig-zag interfacial structure dramatically increased the joint strength. The joint in mode 3 exhibits the highest bending strength of 73 MPa (on average), which is about twice that for mode 2. The effects of the alumina interlayer and zig-zag interfacial structure on the mechanical property of the joint of the C/C-Ni-based superalloy will be discussed in later sections.

3.3.1. Effect of interlayer on the joint strength

The improvement of mechanical strength of the joint in mode 2 over that in mode 1 is presumably due to the reduced residual stress by using the Al₂O₃ interlayer. There are two main aspects that may be responsible for the decreased residual stress in the present study. On one hand, the use of the Al₂O₃ interlayer favours gradual transition of CTE from the C/C to superalloy. As we know, the CTE mismatch is the crucial factor that may induce residual stress. According to the materials supplier, the CTEs (α) for the C/C and superalloy are $(0-2.2) \times 10^{-6}/K$ over 20–2000 °C and $(12.5-16.3) \times 10^{-6}/K$ over 20–1000 °C, respectively. The large CTE mismatches ($\Delta\alpha$) between them will inevitably induce serious thermal stresses at the brazed interface or near the joining region. Al₂O₃ ceramic has a medium CTE of $(7.0-11.4) \times 10^{-6}/K$ over 20–1000 °C. The use of Al₂O₃ interlayer benefits the mitigation of CTE mismatch between the C/C and superalloy and effectively decreases the stress gradient in the joint. Thus, the $\Delta\alpha$ between C/C-Al₂O₃ and Al₂O₃-superalloy

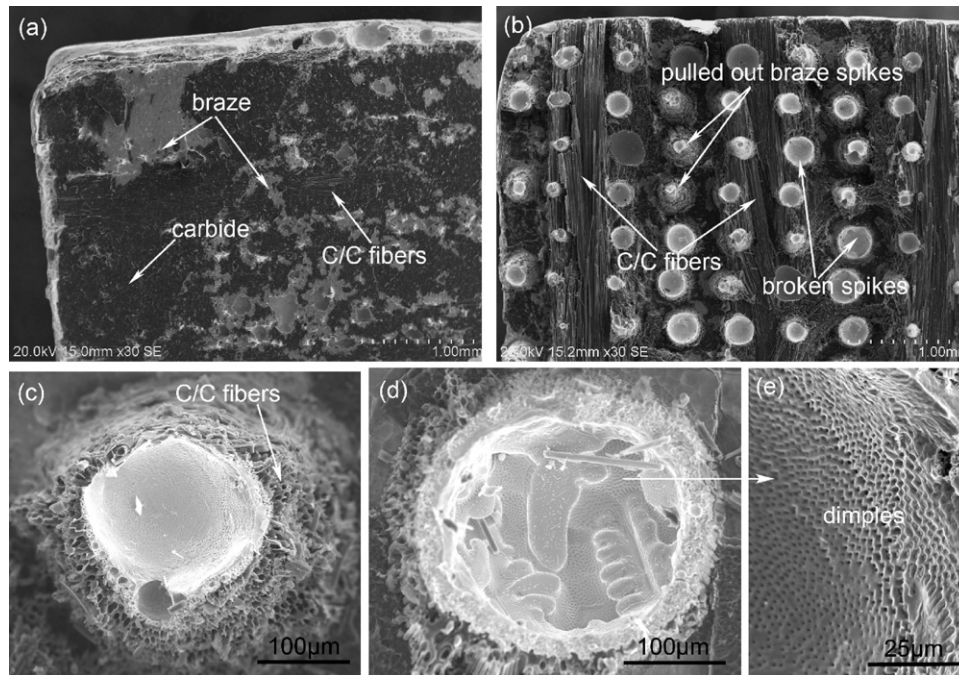


Fig. 6. SEM micrographs of fracture surface on metal side of joint (a) in mode 2 and (b) in mode 3 after mechanical testing.

joints are substantially lower than that of the C/C-superalloy joint. On the other hand, ductile braze interlayer is essentially important for residual stress relief. It is widely accepted that the normal stresses can be sharply reduced when a ductile interlayer with low yield strength (σ_y) is used.^{10,19,20} The σ_y for our braze alloy is measured at about 180 MPa (ductility of 40%). We have noted that the braze in the C/C-Al₂O₃ and Al₂O₃-superalloy joints kept its ductility after brazing. Considering the given CTE values of the joined materials, large thermal strains will occur between them. The thermal strains can be obtained by calculating the $\Delta\alpha\Delta T$, where ΔT is the temperature interval ($\Delta T = 890^\circ\text{C}$). The elastic thermal strains, $\Delta\alpha\Delta T$, for the brazed C/C-Al₂O₃ joint and Al₂O₃-superalloy joint are $\sim 5.3 \times 10^{-3}$ and 4.9×10^{-3} , respectively. These thermal strains are likely to exceed the yield strain of AgCu alloy⁵, indicating that plastic yielding of the braze may happen. The braze interlayer with low σ_y and large ductility will benefit the stress accommodation via its plastic deformation during the cooling process. Contrarily, stress relief will be less effective for a stronger but less ductile braze which shall increase the propensity to crack at the joining interface or in ceramic near the interface. Therefore, due to the serious hardening of the braze interlayer by the brittle compounds in the mode 1 joint, its low joint strength is reasonable.

3.3.2. Effect of interfacial structure on the joint strength

As mentioned above, the joint is further strengthened by the zig-zag interfacial structure. This indicates that interfacial structure also plays an important role in enhancing the joint strength other than reducing the residual stress. It is believed that the micro-machined C/C surface for the mode 3 joint directly resulted in a larger joining area than that of a flat joint by creating a 3D transition region between the C/C and braze after the

holes were fully filled with braze. It is anticipated that the C/C-braze interface in the transition region has less severe residual stress concentration as the ductile braze in the laser machined holes may be helpful to reducing the thermal stress via the plastic distortion of the braze. For a similar case, a rectangular wave interface was created by Xiong et al. for joining C/C to Ti64 alloy²¹. They also found that the level of residual stress at the CC/Ti64 interface in rectangular grooves was lower than that in flat joint. On the other hand, the braze spikes were tightly pinned to the C/C matrix and thus a pinning strengthening effect could be achieved. This effect has been revealed distinctly in joining of C/C^{22,23} or SiC²⁴ to metals using similar machined ceramic surface. Our results show that the micro-machining method is a successful approach to producing high strength C/C-superalloy joint. In general, the factors that have induced mechanical strengthening of the zig-zag interfacial structure may include the enlarged joining area, less severe residual stress concentration and strong pinning effect of the braze spikes.

The SEM micrographs of the fracture surface on the superalloy side of the joint in mode 2 and 3 are shown in Fig. 6. In Fig. 6a, the joint with a flat joining surface shows a flat fracture surface, demonstrating a brittle fracture. The joint cracked at or near the C/C-braze interface. This is the characteristic of fractures in the joints with low strength⁹. By contrast, the joint in mode 3 presents a significantly different fracture, as shown in Fig. 6b. The joint breaks in the transition region between the C/C and the braze. This fracture behaviour has been observed in a C/C-Cu joint using a similar notched joining structure²². A large amount of C/C matrix especially C/C fibre with orientation parallel to the joining interface is attached on the metal side. It means that cracks have propagated into the C/C substrate. Some typical fractures, such as pulling out and breaking of braze spikes are also found. As seen in Fig. 6c, the pulled out braze spikes

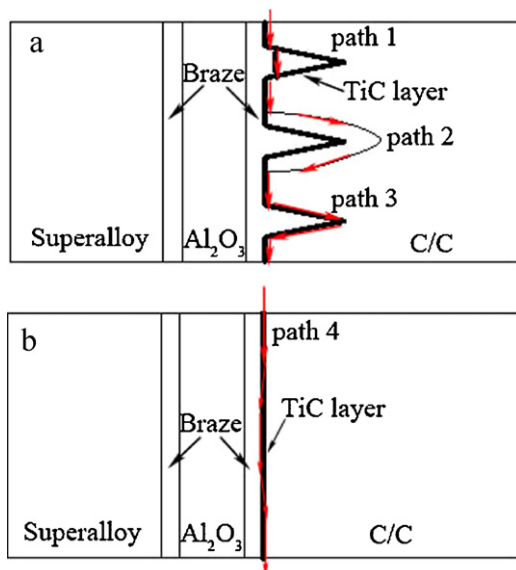


Fig. 7. Schematic of fracture modes for joint (a) in mode 3 and (b) in mode 2.

are surrounded by broken C/C fibres with orientation perpendicular to the joining interface. In addition, dimple-dominated fracture is extensively observed on the fracture surface of the broken braze spike, as illustrated in Fig. 6d and f. It is evident that plastic deformation of braze spikes took place during rupture, which is beneficial to improving the impact resistance of the joint.

The fracture morphology reveals crack propagating path during testing. A schematic of the main fracture modes is illustrated in Fig. 7. For the joint in mode 3, the cracks changed their path as soon as they reached the braze spikes. Thus, the crack paths were well removed from the C/C-braze interface and deflected into the C/C matrix or across the braze spikes. The deflections of the cracks may help to transform the fracture mode from brittle to pseudo-plastic, thus preventing a catastrophic failure. These factors result in increase of propagating path and consuming more energy during the failure, thus enhancing the toughness of the joint.

4. Conclusion

A novel approach to fabricate high strength C/C-superalloy joint was developed using Al_2O_3 as interlayer and/or a zig-zag interfacial structure. Effect of the Al_2O_3 interlayer on microstructure and joint strength and the advantages of the zig-zag interfacial structure were investigated. The results

showed that strength of the C/C-superalloy joint without the interlayer was rather low due to the large residual stress. The joint with the Al_2O_3 interlayer displayed well-bonded interface and ductile microstructure since the diffusion and reactions of Ni and Ti were effectively prevented. The joint strength was improved as a result of the reduced residual stress. Furthermore, the joint strength could be significantly enhanced by the zig-zag interfacial structure. A high strength up to 73 MPa was achieved. The strengthening mechanism was attributed to the enlarged joining area, low residual stress and strong pinning effect of the braze spikes.

Acknowledgement

The authors thank Prof. J.Y. Deng's group for providing C/C samples and Mr. X.F. Mao for technical assistance. Y.X. Shen thanks Drs. C.H. Jiang and J.C. Chen for helpful discussions.

References

- Salvo M, Casalegno V, Vitupier Y, Cornillon L, Pambaguian L, Ferraris M. *J Eur Ceram Soc* 2010;**30**:1751–9.
- Hutton TJ, McEnaney B, Crelling JC. *Carbon* 1999;**37**:907–16.
- Merola M, Akiba M, Barabash V, Mazul I. *J Nucl Mater* 2002;**307**:311:1524–32.
- Qin YQ, Feng JC. *Mater Sci Eng A* 2007;**454–455**:322–7.
- Singh M, Shpargel TP, Morscher GN, Asthana R. *Mater Sci Eng A* 2005;**412**:123–8.
- Singh M, Asthana R, Shpargel TP. *Mater Sci Eng A* 2007;**452–453**:699–704.
- Moutis NV, Jimenez C, Azpiroz X, Speliotis Th, Wilhelmi C, Messoloras S, Mergia K. *J Mater Sci* 2010;**45**:74–81.
- Singh M, Asthana R, Shpargel TP. *Mater Sci Eng A* 2008;**498**:19–30.
- Xian AP, Si ZY. *J Mater Sci* 1992;**27**:1560–6.
- Galli M, Botsis J, Janczak-Rusch J. *Adv Eng Mater* 2006;**8**:197–201.
- Park JW, Mendez PF, Eagar TW. *Acta Mater* 2002;**50**:883–9.
- Hattali ML, Valette S, Ropital F, Stremsdoerfer G, Mesrati N, Tréheux D. *J Eur Ceram Soc* 2008;**29**:813–9.
- Gotman I, Gutmanas EY. *Acta Metall Mater* 1992;**40**:S121–31.
- Van der Eijk C, Sallom ZK, Akselsen OM. *Scripta mater* 2008;**58**:779–81.
- Grummon DS, Shaw JA, Foltz J. *Mater Sci Eng A* 2006;**438–440**:1113–8.
- Koltsov A, Hodaj F, Eustathopoulos N. *J Eur Ceram Soc* 2009;**29**:145–54.
- Asthana R, Singh M. *J Eur Ceram Soc* 2008;**28**:617–31.
- Xiong JT, Li JL, Zhang FS, Huang WD. *Scripta Mater* 2006;**55**:151–4.
- Levy A. *J Am Ceram Soc* 1991;**74**:2141–7.
- Hattali ML, Valette S, Ropital F, Mesrati N, Tréheux D. *J Mater Sci* 2009;**44**:3198–210.
- Xiong JT, Li JL, Zhang FS, Lin X, Huang WD. *Mater Sci Eng A* 2008;**488**:205–13.
- Schedler B, Huber T, Friedrich T, Eidenberger E, Kapp M, Scheu C, Pippan R, Clemens H. *Phys Scr* 2007;**T128**:200–3.
- Wang HQ, Cao J, Feng JC. *Scripta Mater* 2010;**63**:859–62.
- Südmeyer I, Hetteshheimer T, Rohde M. *Ceram Int* 2010;**36**:1083–90.